Seismological Research Letters Volume 71, Number 4, 423-436 July/August 2000

A Transportable System for Monitoring Ultra Low Frequency Electromagnetic Signals Associated with Earthquakes

Darcy Karakelian, Simon L. Klemperer, Antony C. Fraser-Smith, and Gregory C. Beroza
Stanford University, Department of Geophysics, Stanford, CA 94305-2215
darcy@pangea.stanford.edu

INTRODUCTION

Claims that electromagnetic (EM) signals occur associated with some earthquakes, typically prior to but sometimes during seismic activity, have appeared in the literature for several decades (Parrot and Johnston, 1989; Park, *et al.*, 1993; Park, 1996; Johnston, 1997). Such claims cover an exceptionally broad range of phenomena. For example, Gokhberg *et al*. (1982) and Yoshino (1991) observed increases in signal amplitude at 81 kHz from minutes to hours prior to earthquakes and up to hundreds of kilometers away from epicenters, and attributed these signals to seismoelectric emissions. Seismoelectric signals (SES) of a different nature have been suggested to precede some earthquakes in Greece (Varotsos *et al*., 1993a; Varotsos *et al*., 1993b). These SES are transients of amplitudes of 20 mv/km and durations of several minutes recorded on multiple dipoles of different length, and their mechanism of generation is subject to debate (Lighthill, 1996; Pham *et al.*, 1999).

Reported claims of EM anomalies associated with earthquakes also extend over a large frequency range, from megahertz down to quasi-dc. At the low end of the

frequency range, Johnston and Mueller (1987) observed magnetic field offsets coinciding with the 1986 North Palm Springs earthquake, which occurred in Southern California close to the San Andreas Fault, and Johnston *et al.* (1994) also observed offsets at the time of the 1992 Landers earthquake in the same region. At the high frequency end, radio emissions at 18 MHz were recorded on multiple northern hemisphere receivers for about 15 minutes before the 1960 great Chilean earthquake (Warwick *et al.*, 1982). In the ULF (0.01-10 Hz) frequency range, Fraser-Smith *et al.* (1990) recorded anomalous magnetic field fluctuations prior to the 10/17/89 Loma Prieta M_s=7.1 earthquake in central California. In particular, there was an amplitude increase in activity about two weeks prior to the main shock that continued until an even larger-amplitude increase starting three hours before the main shock. Other anomalous ULF emissions possibly related to earthquakes were recorded several hours prior to the 12/7/88 M_s=6.9 Spitak, Armenia, earthquake (Molchanov *et al.*, 1992, Kopytenko *et al.*, 1993), and further anomalous emissions were observed both about two weeks and a few days before the 8/8/93 M_s=8.0 Guam earthquake (Hayakawa *et al.*, 1996).

Most suggested precursory earthquake anomalies were recorded serendipitously by observing systems established for other purposes, and they lack the simultaneous corroborative observations on identical but spatially separated measurement systems, and/or the long-term recorded time series on each individual system, that are necessary to exclude other potential sources of EM activity and so to establish the credibility of the claims. Some dedicated long-term observatories have been established, particularly in Greece (Varotsos *et al*., 1993a), Japan (Uyeda *et al*., 1998), and the USA (Johnston, 1989; Park, 1991) to address these credibility issues. However, permanent EM

observatories may require researchers to wait for decades for the occurrence of even one sufficiently large, sufficiently close, earthquake to test whether that earthquake had associated EM signals (preseismic, coseismic, or postseismic). Because a repeat observation of similar EM anomalies from a repeat earthquake will require maintenance of a permanent observatory during an entire earthquake cycle, complete verification of the existence of EM earthquake anomalies, should they exist, is unlikely in our lifetimes.

We have therefore designed a transportable recording system for rapid deployment in the epicentral region of a major earthquake immediately following a main shock. Placing at least three recorders in the aftershock region of a major earthquake will allow us the opportunity to record both continuing EM activity due to the main shock and its post seismic response, as well as precursory and/or coseismic EM signals associated with aftershocks, should any or all of these phenomena occur. Although in this recording mode we may not be able to distinguish preseismic from postseismic EM activity, the widely accepted detection of any earthquake-associated EM signal would represent a fundamental advance in our knowledge of earthquake physics.

We have focused our attention on the ULF part of the EM spectrum, to which increasing attention has been drawn since the recording of unusual ULF magnetic signals prior to the Loma Prieta earthquake (Fraser-Smith *et al*., 1990 and 1993; Bernardi *et al*., 1991) for which multiple, but not mutually exclusive, possible physical explanations have been given (Draganov *et al*., 1991; Fenoglio *et al.*, 1995; Merzer and Klemperer, 1997). In addition to these and the other ULF anomalies previously mentioned, the ULF band is worthy of attention because these signals can be recorded at the earth's surface without significant attenuation if they are generated at typical earthquake nucleation depths (~10

km). Higher frequencies, in the VLF band, would have smaller skin depths[1] and therefore greater attenuation before reaching the earth's surface (Telford *et al.*, 1990, Chp. 6).

It is not possible to demonstrate that any recorded ULF anomaly is truly generated by an earthquake because the earthquake process cannot be experimentally reproduced. Rather, one must judge the claim that a measured anomaly is associated with an earthquake based on three criteria: simultaneous recording on multiple independent instruments, the reliability of the instruments, and the plausibility of the scientific model that accounts for it. Developments in the field of earthquake electromagnetics therefore require advances on two fronts: improvements in the quality and quantity of instrumentation, and improvements in our understanding of physical processes preceding earthquakes. In this paper we focus only on the former issue, the development and installation of appropriately sensitive and reliable recording instruments. We describe the sensors and recorders we are using, the installation methods we have found efficient but reliable, and the type and quality of data that results in a manner similar to that provided by Uhrhammer *et al.*, (1998) for broad-band seismic station installation.

STANDARDS FOR DATA COLLECTION

In order to isolate ULF signals of tectonic origin, we need to characterize and minimize other sources of ULF signals in the vicinity of our portable station. These other sources include ionospheric/magnetospheric geomagnetic variations, cultural interference, signals

[1]An EM wave is attenuated by a factor *e* after transmission through one skin depth, δ, where $\delta = (2\pi f\mu\sigma)^{-1/2}$. For frequency f = 0.1 Hz, magnetic permeability $\mu = \mu_o = 4\pi * 10^{-7} Hm^{-1}$, and upper-crustal conductivity σ = 0.01 Sm^{-1}, δ = 10 km.

induced in the equipment due to movement, temperature and other environmental variables, and instrument noise. These sources will influence the choice of location for the EM station as well as the variety of instruments that are deployed. Ideally, a portable ULF EM station should measure 3 components of the magnetic field and 2 components of the electric field in 2 separate locations a minimum of several km apart, and it should be collocated with a seismic station and also possibly a tiltmeter to identify displacements and rotations of the sensors during earthquakes.

Figure 1 shows the spectrum of typical background geomagnetic activity at a mid-latitude location. The predominant background signals we measure at an EM station are natural signals generated in and above the ionosphere including Schumann resonances, natural radio emissions from lightning strokes, and variations in the geomagnetic field. Variations in the geomagnetic field, which are largely governed by the activity of the sun, include daily magnetic variations, geomagnetic storms, and pulsations (including the low frequency Pc pulsations). These global phenomena produce a variety of signals ranging in frequencies from 10^{-3} Hz to 10^{6} Hz, and with amplitudes on the order of a few nT, although geomagnetic storms can produce signals as large as 30 nT (see e.g. Tascione, 1994). A typical feature of the spectrum of ULF geomagnetic activity shown in Figure 1 is a minimum of activity in the interval 1-7 Hz (*c.f.* Campbell,1969, and Fraser-Smith and Buxton, 1975). At higher frequencies, the first Schumann resonance produces an increase in geomagnetic activity at frequencies in the range 6-9 Hz. At lower frequencies, there is no minimum of activity between the different classes of Pc pulsations, despite their different properties (Jacobs, 1970), and we see a monotonic increase of activity with decreasing frequency throughout the frequency range 3-0.01 Hz.

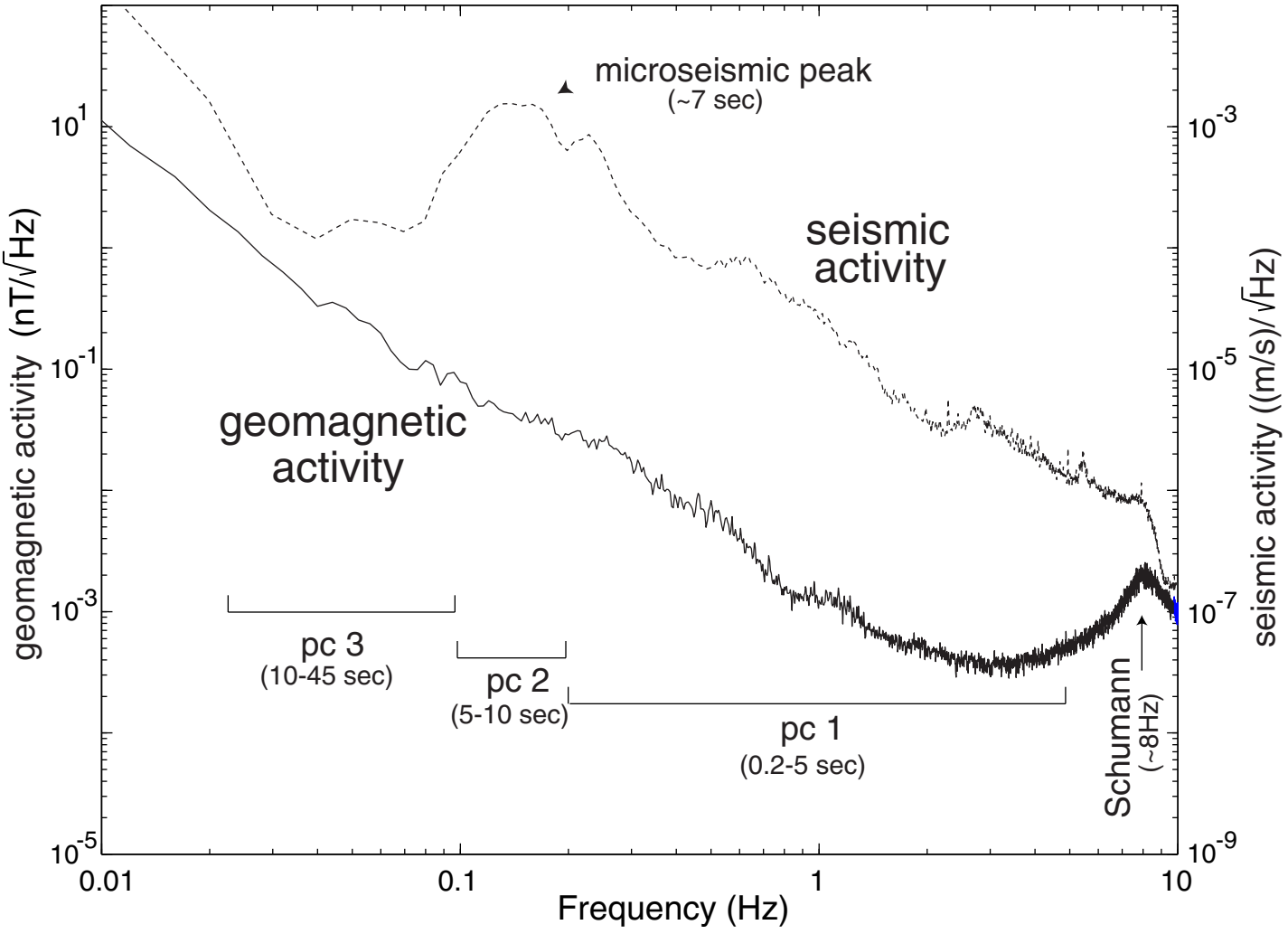

Figure 1. Representative power spectra of typical geomagnetic activity (solid curve) and corresponding broadband seismic activity (dashed curve) recorded near Hollister, CA on May 2, 1998. The predominant sources of geomagnetic activity, including pc 1, pc 2, and pc 3 geomagnetic pulsations, and the fundamental Schumann resonance, are shown. (Data courtesy of the Northern California Earthquake Data Center, and the Berkeley Seismological Laboratory and the University of California, Berkeley, CA)

Larger-scale variations can be reduced in these data using a remote station typically 10 to 100 km distant. Temporary EM deployments in California can use an existing array of continuously recording permanent EM stations as remote sites for the reduction of geomagnetic disturbance signals (Figure 2A). In addition to a remote reference, any portable deployment should utilize two or more stations deployed a few kilometers apart (a separation of similar magnitude to the hypocentral depth or fault length). The existence of data from two fairly close sites not only allows for the removal of geomagnetic variations in the data, but may provide duplicate recordings of anomalous signals, enhancing their credibility, and yielding information about the spatial variation of any observed anomalies.

Although not as sensitive as a broadband seismometer, a ULF magnetic induction coil is responsive to microradian tilts (a broadband seismometer is typically capable and responsive to sub-nanoradian tilts (Uhrhammer *et al*., 1998)), and it is impossible to distinguish the effect of ground motion from real variations of the magnetic field. In order to reduce movement from environmental variables such as wind, care is taken to bury the sensors in open spaces (see **Deployment** section). However, because we are interested in measuring signals of tectonic origin, co-located broadband seismic recordings are necessary to establish whether observed signals are due to ground motion. Typical seismic background activity (Figure 1) shows a ~7 s "microseismic" peak, presumably induced by distant ocean waves (Longuet-Higgins, 1950), which has a lower amplitude than is detectable by most magnetic sensors; but large local earthquakes undoubtedly produce tilts that induce significant magnetic fields (Bernardi et al., 1991).

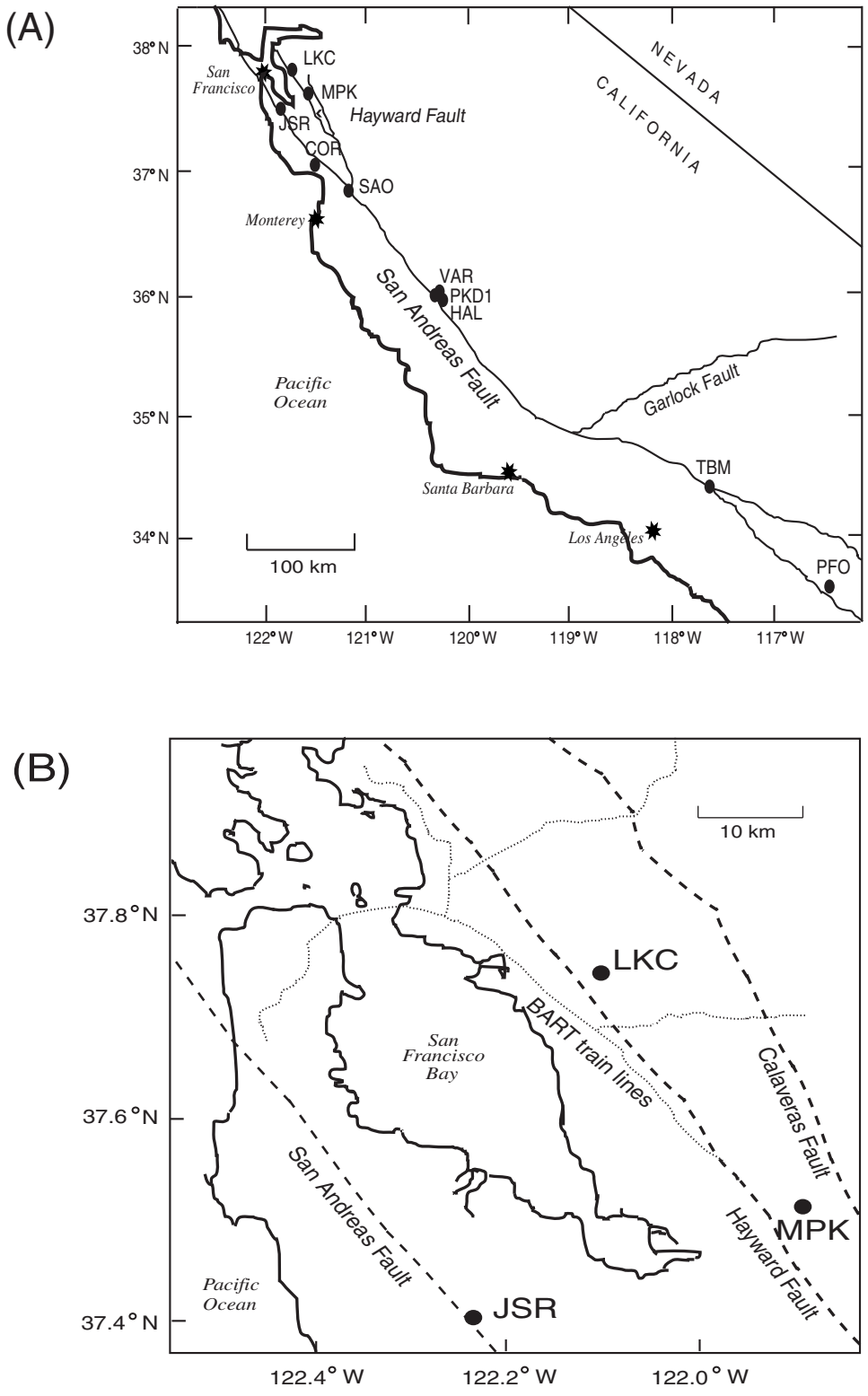

Figure 2. A. Map showing the location of California-wide ULF stations. PKD1 and SAO are operated by Dr. H.F. Morrison and colleagues at the University of California, Berkeley. All others are operated by Stanford University. B. Map showing JSR and other San Francisco Bay Area ULF stations with respect to local faults (dashed lines) and BART train lines (dotted lines).

Unlike the thermal sensitivity of a broadband seismometer, temperature variations are not a significant source of noise in our electric and magnetic field sensors. Shallow burial insulates the sensors from any measurable short-term thermal noise, even in the most extreme temperature environments.

The existence of cultural electromagnetic noise, such as power lines, DC railways, automobiles, etc., provides the largest challenge when trying to isolate signals of tectonic origin. These sources of interference vary in frequency and are local in nature, so they can be difficult to distinguish from anomalous signals of tectonic origin. In order to understand and characterize this cultural noise, it is important to establish a library of continuous records from a specific location. To reduce this interference, EM stations should be deployed at remote sites, and data analysis should focus on hours when cultural noise is significantly reduced, i.e. in the middle of the night.

Finally, a transportable system must be readily available in the event of a major earthquake with the ability to transport and install the entire system within, say, 48 hours.

INSTRUMENTATION FOR STANFORD PROTOTYPE TRANSPORTABLE SYSTEM

Our system employs BF-4 and BF-21 Magnetic Field Induction Sensors manufactured by Electromagnetic Instruments Inc. (EMI)[2]. Each sensor contains a coil and a low-noise pre-amplifier sealed inside a waterproof, impact resistant Nema G-10 fiberglass tube. Two BF-4 sensors measure the horizontal east-west and north-south components of the magnetic field, and a BF-7 sensor measures the vertical component of the magnetic field.

[2] Electromagnetics Instruments, Inc. (EMI), Richmond, CA, USA, *http://www.emiinc.com*

Sizes and weights are shown in Table 1. Our vertical sensor is shorter than the horizontal sensors allowing greater ease of burial in the vertical position. The BF-7 vertical sensor has recently replaced the BF-21 sensor of essentially identical sensitivity (Table 1). Amplitude/phase response and system noise characteristics are specified over the frequency range 0.0001 Hz to 1000 Hz (Figure 3).

TABLE 1
Sizes and Weights of Magnetic Field Induction Sensors

	Length	Diameter	Weight
BF-4 (horizontal)	142 cm	6 cm	7.9 kg
BF-7 (vertical)	104 cm	6 cm	7 kg
BF-21[a]	63 cm	16 cm	22 kg

a. no longer manufactured

The electric field measurement component consists of an EMI two-channel electric field signal conditioner (EFSC) rated from 0.001 Hz to 3000 Hz with a 0.001 Hz highpass filter. This instrument is highly portable, weighing about 3 kg in an ABS waterproof case. Three low-frequency, non-polarizable Pb-$PbCl_2$ electrodes (EMI) designed for low noise and low dc drift are used to measure two orthogonal components of the electric field. However, in order to distinguish between electrode noise and earth signals, it would be better to use a fourth, rather than a common electrode. Redundant electrodes, virtual dipoles, and/or an independent diagonal dipole are various schemes recommended to verify that observed signals have constant voltage to distance ratios, as expected from an electric field disturbance (Roeloffs *et al*., 1996).

Rugged construction of both the induction coils and the electrodes allows for complete burial underground for protection against temperature variations and wind

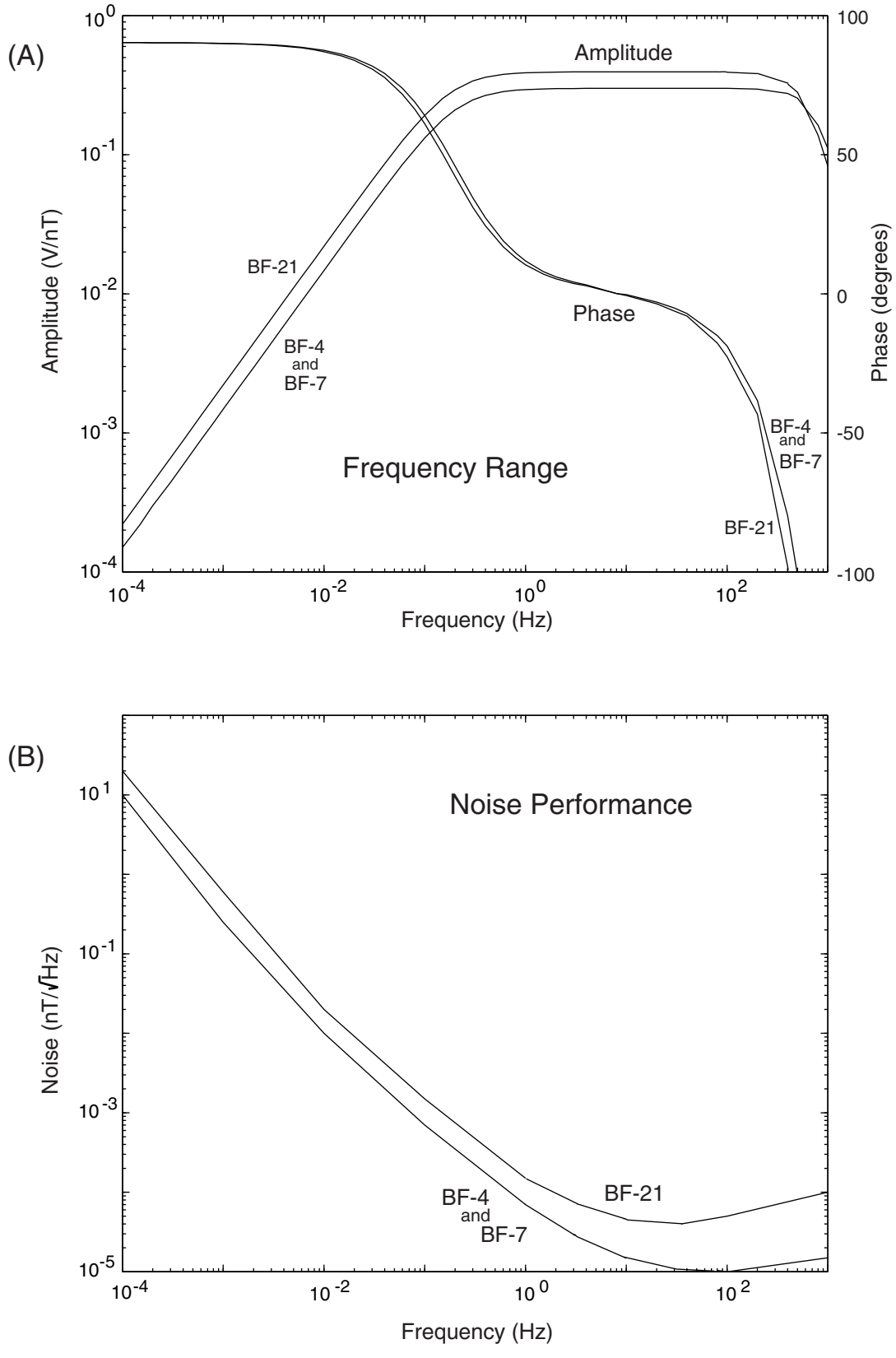

Figure 3. Amplitude/phase and system noise characteristics of the EMI BF-4 and BF-21 induction coils used at JSR. (Courtesy of Electromagnetic Instruments, Inc.)

noise. In addition, all cable connectors to the sensors are waterproof. Figures 4A and B show the magnetic induction coils and the electric field signal conditioner with an electrode, respectively.

Total power consumption for the 5 component system is less than 2 A-hr/day. Our system is powered in the field by six 80 A-hr gel-cell batteries. These batteries provide at least 2 months of continuous power.

Data Acquisition

We are using two, 3-channel 72A-07 High Resolution Digitizers manufactured by Refraction Technology, Inc.[3] provided by Stanford University and the IRIS PASSCAL Instrument Center[4]. These 24-bit digitizers can accept 20 V peak-to-peak, differential input (at unit gain) and store up to 1 GB on their internal hard drives (≈ 2 months of 3-channel data at 40 sps). An internal crystal clock provides real time to 5 x 10^{-7} accuracy and is phase-locked to an internal GPS Receiver. Field recording parameters are downloaded to the digitizer from a laptop. Data are continuously recorded at a 40 Hz sample rate and can be downloaded in the field using PASSCAL software and stored on tape for further analysis.

The Reftek Digitizer is compact (32 x 21 x 20 cm), watertight, and lightweight (5.5 kg). The typical power requirements for a field site are 4 W continuous at 12 V DC. For a portable deployment, one 80 A-hr battery will supply 10 days power for one Reftek.

[3] Refraction Technology, Inc. (REF TEK), Dallas, TX, USA, *http://www.reftek.com*
[4] IRIS PASSCAL Instrument Center, Socorro, NM, USA, *http://www.passcal.nmt.edu*

(A)

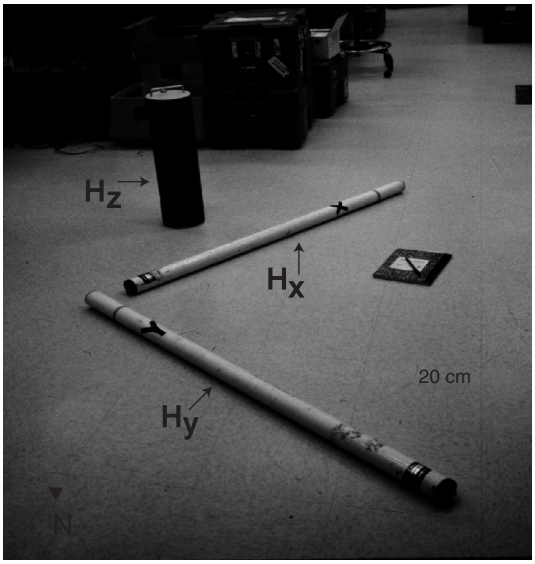

(B)

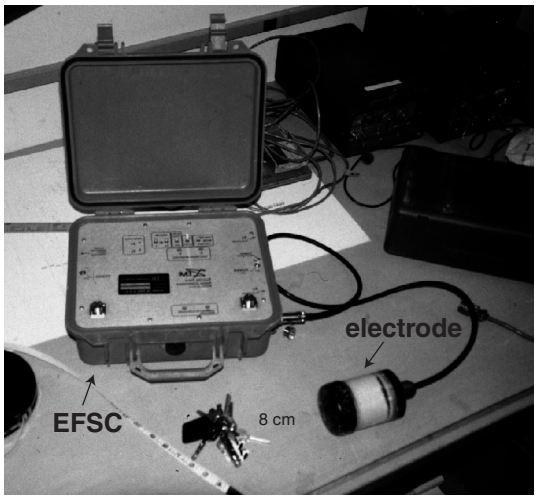

(C)

Figure 4. Pictures of the equipment used at JSR before and during the installation. A. Induction coils, H_x, H_y, and H_z (upright). B. Pb-PbCl electrode connected to the electric field signal conditioner. C. BF-4 coil enclosed in PVC pipe during burial in the field.

DEPLOYMENT METHODOLOGY FOR THE STANFORD TRANSPORTABLE SYSTEM

Deployment of equipment in an efficient and timely manner is an essential aspect of a short-term deployment project and is, consequently, a key focus of this paper. Details of the installation of a 5-component transportable ULF EM recording system, including proper burial, housing of the equipment, and time/labor/cost requirements are important considerations on which the optimal operation of our equipment, and consequently the credibility of our field measurements, will depend.

Deployment of the Induction Coils

Burial of the three EMI induction coils minimizes noise due to weather induced movement and temperature variations. The induction coils are buried about 15-20 ft apart and oriented in geographic E-W (H_x), N-S (H_y), and vertical (H_z) directions using a Brunton compass and a level bubble. The horizontal BF-4 sensors are completely enclosed in 3" PVC pipes with endcaps (Figure 4C). The PVC pipe is padded with foam on the inside to increase stability of the sensor. (These pipes also make durable shipping cases.) Each sensor should be leveled with a level bubble and buried at least 1 ft deep. It is important to surround the PVC pipe with loose dirt, that will pack tighter than larger clumps during burial, to minimize any movement due to settling of the surrounding earth. Once the sensor is completely buried, care should be taken not to step around the area or otherwise disrupt the sensor's alignment. Concrete blocks are placed at the end of the coils to mark their position. The coils should be buried as deeply as possible to avoid

external noise due to wind and rain, and away from large trees whose root systems may move in windy conditions causing ground movement.

The vertical sensors (H_z) require a three-foot (or deeper) vertical hole (a two-person hand auger may be necessary in hard soil). The sensor can be directly buried in the ground or enclosed in PVC pipe for additional protection, and leveled with a level bubble. If enclosed in PVC, drainage holes should be drilled in the bottom of the vertical sensor pipe to prevent water build up.

The cables connecting the coils to the power supply must be completely buried underground to avoid movement of the coils and damage by animals. The sensor cables, enclosed in 1.5" PVC piping, surface at the EMI coil power supply box (BFPS) and batteries, which are placed at the maximum distance that the cables allow. From the BFPS the sensor output cable is fed a minimum of 50 m away to the Reftek and GPS antenna.

Ideally, the Reftek and its batteries should be protected from the elements, perhaps in a plastic tote-box, and if necessary buried or hidden to avoid human disturbance. Solar panels may be required for power if sufficient batteries or a line power supply are not available. The Refteks and power supplies should be safely secured to ensure continuous recording throughout any earthquake.

Deployment of the Electric Field Measurement System

The electric field measurement system includes three identical electrodes buried in a triangular fashion, laid out in geographic E-W (E_x) and N-S (E_y) directions. Electrodes should be buried ~100 m apart from each other to maximize the earth signal to electrode

noise ratio. At the bottom of a 1 ft (or deeper) hole, water, clay (bentonite is recommended), and dirt are combined until a thick mud mixture is created. The electrode is then placed into this mixture (almost completely buried) and loose dirt is added carefully until covered. It is important that loose dirt is used to cover the remainder of the electrode rather than large clumps to ensure the best coupling. The remainder of the hole is then completely filled. Although it is not known what effect, if any, a difference in elevation has on the output signals, we attempt to bury the electrodes at a common level. The electrode cables and piping (again, recommended but not essential) are joined together at a plastic tote-box sitting about 1 ft away from the buried common electrode from which a single sensor cable will be fed out to a separate Reftek. The box contains the batteries, signal conditioner, and any extra cabling and is partially buried to ensure stability. Drainage holes are drilled in the bottom of the plastic box to avoid water build up. A plastic tarp thrown over the box is an effective extra waterproofing precaution.

Time/Labor/Cost Requirements

Although we prefer to enclose all cables in PVC pipe and bury them when necessary, this increases the time and labor involved and may not be feasible for a short-term installation. In the event of a short-term deployment, the induction coils as well as the sensor cables can be buried directly in the ground. Three field assistants can realistically deploy the entire system in less than one day.

A total of six 80 A-hr. gel cell batteries is adequate to supply the electrodes and induction coils with power for at least two months in the field. However, each 3-channel

Reftek requires a new 80 A-hr battery every ten days, so that solar panels are preferred for a portable deployment.

Expenses, excluding any of the equipment listed in the instrumentation section of this paper, will include transportation costs, power supply costs (batteries or solar panels) and any field tools and piping required. Expenses for the deployment of our prototype system, a local but semi-permanent installation (see **Case Study** section) were less than $300.00.

CASE STUDY: DATA FROM OUR PROTOTYPE SYSTEM

In order to develop reliable and efficient procedures for rapid deployments, to gain experience in data analysis, and above all to trouble-shoot the combined EM/seismic system, we have installed a prototype of this portable recording system at Jasper Ridge Biological Preserve (site JSR) on Stanford University's campus. We chose Stanford lands not only to carry out our initial experimentation but also to use as a "parking array" for the equipment when not in use for an aftershock study. The accessibility of the site has enabled us to install, maintain, and monitor the equipment on a continuous basis over the last year. JSR was set up as a semi-permanent station from which the equipment can be removed at a moment's notice, or which can continuously record for months at a time without interruption.

The JSR station (37.404º N, 122.238º W) is located 6 km southwest of Stanford University in the foothills of the Santa Cruz Mountains (see Figure 2B). The equipment is buried in surficial, alluvial sediments, above Franciscan greenstone, with a serpentine wedge located northeast of the array (Dibblee, 1966). Although Jasper Ridge is not free

from EM interference, it is a protected site conveniently close to Stanford and is less than 1 km northeast of the San Andreas Fault, which we are therefore continuously monitoring for ULF activity.

The predominant source of EM interference at JSR is BART (Bay Area Rapid Transit), a 1000 V DC electric railway that serves the San Francisco Region (Figure 2B). A single BART train may draw up to 10,000 A during maximum acceleration (Liu and Fraser-Smith, 1997). Current returns to the substations primarily through the running rails which are well insulated, but some current does return through the Earth. Although the closest BART station is 30 km away, this leakage current gives rise to signals that dominate our magnetic and electric field records.

Another possible source of local noise is a 26 V DC power line that runs underground, only about 20 m away from E_y, the southernmost electrode in the array. There is a parking lot about 30 m from E_x, although vehicle traffic is limited and rarely exists in the evenings. The Stanford Linear Accelerator Center (SLAC), only 1 km north of the Jasper Ridge system, operates at 120 Hz (Phil Burrows, personal communication) and has no recognizable effect on our records.

Figure 5 shows a block diagram of the three-axis magnetic field and two-axis electric field measurement system at JSR. All five components are recording data on a continuous basis. The time series of the magnetic and electric field data are digitized and stored at the site and require monthly dumps to tape for further analysis. The JRSC seismic station, one of over 20 seismic stations maintained by the Berkeley Digital Seismic Network (BDSN) (*http://quake.geo.berkeley.edu/bdsn/bdsn.overview.html*) and the University of California, Berkeley, is also located at this site. JRSC employs a

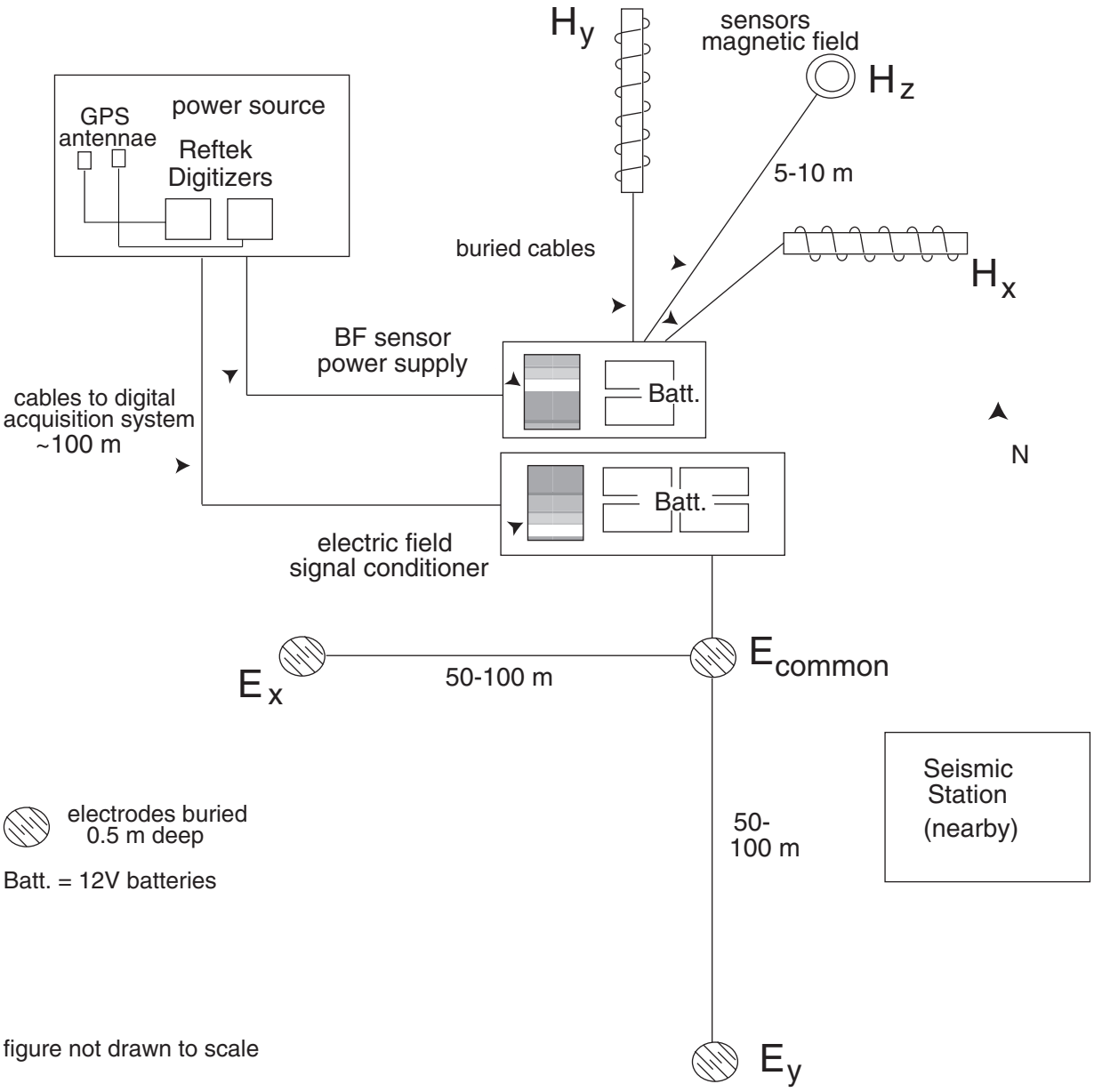

Figure 5. Block diagram of the equipment at a typical ULF station. At JSR, a shed with direct line power houses the data acquisition system. In addition, a broadband seismic station is located about 20 m away from the magnetic sensors.

Streckeisen, AG, STS-2 broad-band triaxial seismometer and a 24-bit Quanterra Q680 digital data logger. The instruments are contained in an aluminum pressure tank set on a concrete pier, in a vault located in a 6 m-long east-west adit. Approximately 4 m of overburden covers the adit, which is 20 m south of our induction coils.

The installation at JSR closely followed the deployment guidelines described above. However, although it is a convenient location to house our equipment when not in use for a portable deployment experiment, JSR is limited in terms of topography and space and is therefore not ideal for this type of installation. For example, the electrodes should be spread further apart (100 m rather than ~50 m possible at JSR), and the electrodes should be placed at relatively the same level (at JSR the common electrode is buried ~10 m higher than E_x and E_y).

To date, the most significant problems we have encountered with the JSR array have been water related: wet connections substantially increase system noise. All of the EMI equipment and cables/cable connectors that we are using are waterproof; however, caution must be taken when adding outside components to the system, such as external power supplies.

During this development stage of our project, we need to build up a library of continuous records in a variety of weather conditions, magnetic fluctuations, and cultural interference so that we can better understand potential sources of variations in the magnetic and electric fields. Figures 6A and B show typical spectrograms of the magnetic and electric fields, respectively, recorded on all components at JSR over a typical 3 day period. Figure 6C shows geomagnetic activity, measured by Kp indices, which range from 0-9 and represent an average value of a quasi-logarithmic index,

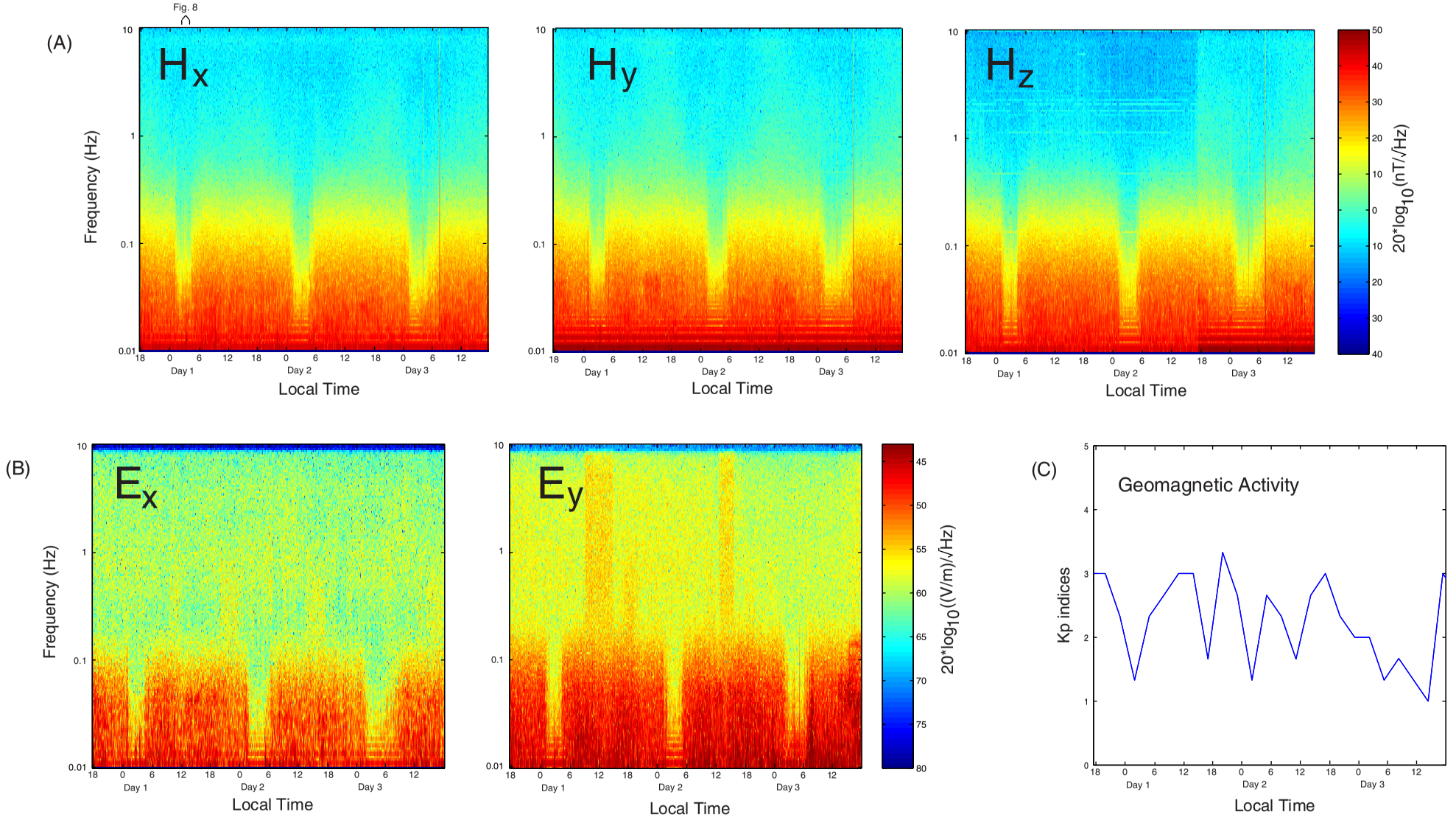

Figure 6. Spectrograms of data recorded at JSR over a typical 3 day period. A. Relative amplitude of magnetic field data recorded on Hx, Hy, and Hz. All magnetic data is equally scaled and plotted in units of 20*log10(nT/ÖHz). B. Electric field data recorded on Ex and Ey, equally scaled and plotted in units of 20*log10((V/m)/ÖHz) . C. Geomagnetic activity (Kp indices) for the same 3 day interval.

measured at 13 geomagnetic observatories, of the 3-hourly range in magnetic activity (Tascione, 1994). The geomagnetic activity is low (Kp index ≈3) and remains relatively constant over the 3 day period displayed.

In Figures 6A and B, there is a reduction in the signal at lower frequencies during approximately 2-4 am local time coinciding with the few-hour interval when BART is not running. Daytime magnetic field activity at JSR is clearly dominated by BART disturbances, which range in amplitude from 0.5 to 3 nT and have characteristic time scales of 5 to 20 sec (Fraser-Smith and Coates, 1978; Liu and Fraser-Smith, 1998). We expect the early morning (BART off) signal to be slightly higher on the horizontal components (H_x and H_y) than on H_z, especially when there is particularly high geomagnetic activity, because natural atmospheric sources create EM plane waves propagating through the atmosphere. On the other hand, there may be stronger broadband activity on H_z than on H_x and H_y during BART operation as expected for BART leakage currents that are dominantly horizontal at our large distance (~30 km) from their source.

Expectations regarding the electric field measurements (Figure 6B) are few, as these are the first continuous measurements of this type made in the Bay Area. We can confirm that the electric field measurements are sensitive to BART, and we can also see enhanced broadband activity on E_y, the dipole located closer to cultural signals at JSR, (i.e. E_y is physically located closer to the main scientific office at Jasper Ridge, as well as to the underground power line), most pronounced around midday local time.

The sensitivity and response of our instruments to both natural and artificial noise, especially BART, is shown in Figure 7, in which the representative amplitudes of H_x and H_z are displayed. Both plots show instrument noise of the EMI induction coils,

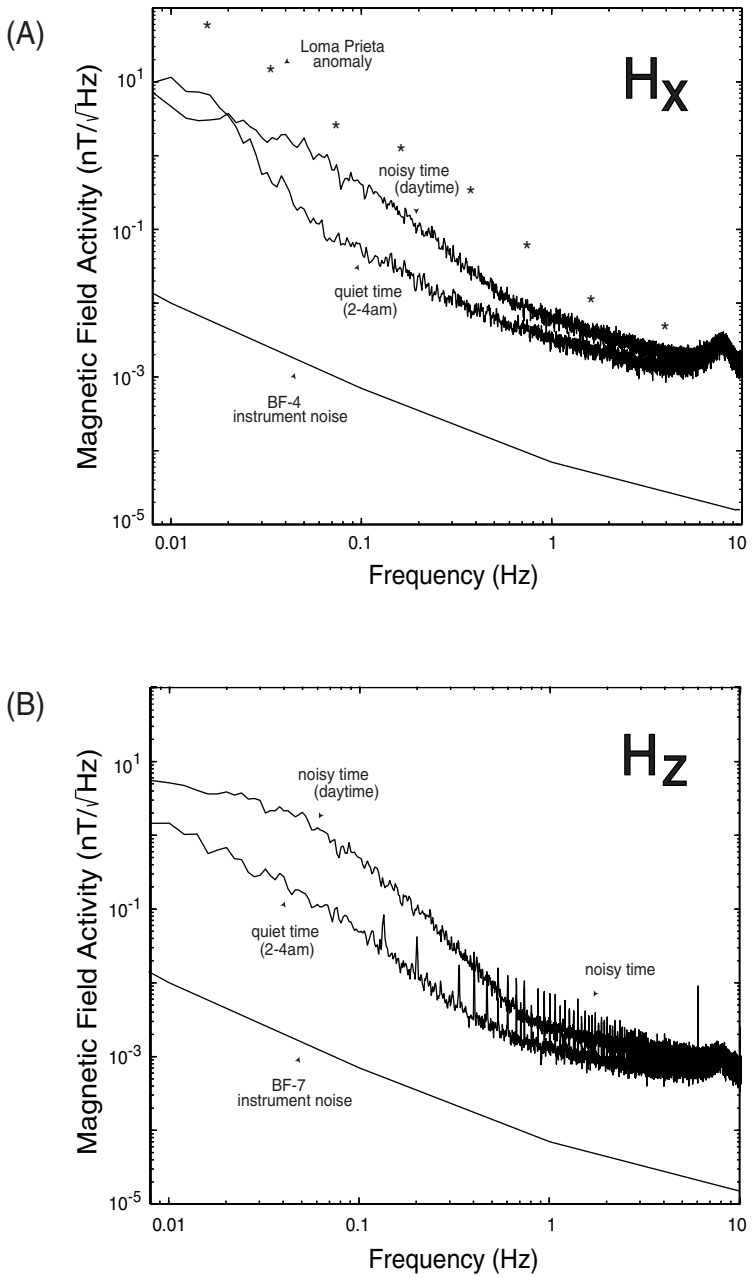

Figure 7. Representative power spectra of typical background magnetic field activity measured from JSR for Hx (A) and Hz (B). Curves are manufacturer-specified instrument noise of the EMI induction coils, background noise during a quiet time (2:00-4:00 am local time), and background noise during a more noisy time when BART is running. Asterisks in A are peak magnetic activity measured within the two week period prior to the Loma Prieta 1989 earthquake (Fraser-Smith et al., 1990).

background activity during a quiet time (2:00-4:00 am local time), and background activity during a more noisy time when BART is running. The peak magnetic activity measured within the two week period prior to the 1989 Loma Prieta earthquake as recorded at Corralitos, CA (Fraser-Smith *et al*., 1990) is also plotted in Figure 7A. At 0.1 Hz, the Loma Prieta signal is almost 50 times greater than that measured at quiet times, and is almost 5 times greater than that measured at a particularly noisy time. Although infested with BART signals, our measurements are clearly sensitive to anomalies on the order of those observed prior to the Loma Prieta earthquake.

At 0.1 Hz, the frequency around which most BART signals are centered, H_x and H_z are about an order of magnitude greater during BART operation hours than during quiet times. During these quiet times, when the signals we measure are predominantly atmospheric in nature, H_x is stronger than H_z at the lower frequencies. This probably reflects the higher sensitivity of the horizontal components to low frequency ionospheric disturbances, a phenomena which can be clearly seen on the plots around 8 Hz where the Schumann resonance peak is more clearly defined on H_x than on H_z. However, there is a greater noise on H_z between 0.3 and 3 Hz, most likely due to cultural interference to which H_z is expected to be more sensitive.

Finally, we compare two hours of data from SAO, an EM station using identical induction coils about 130 km southeast of JSR (Figure 2A), to that collected at JSR. The raw time series traces shown in Figure 8A were recorded at 40 samples per second from 2:00 to 4:00 local time on H_x at both stations and show excellent higher-frequency waveform correlation between the two stations. The equivalent power spectra (Figure 8B) also show good correlation. The higher noise observed at JSR between 1 and 5 Hz

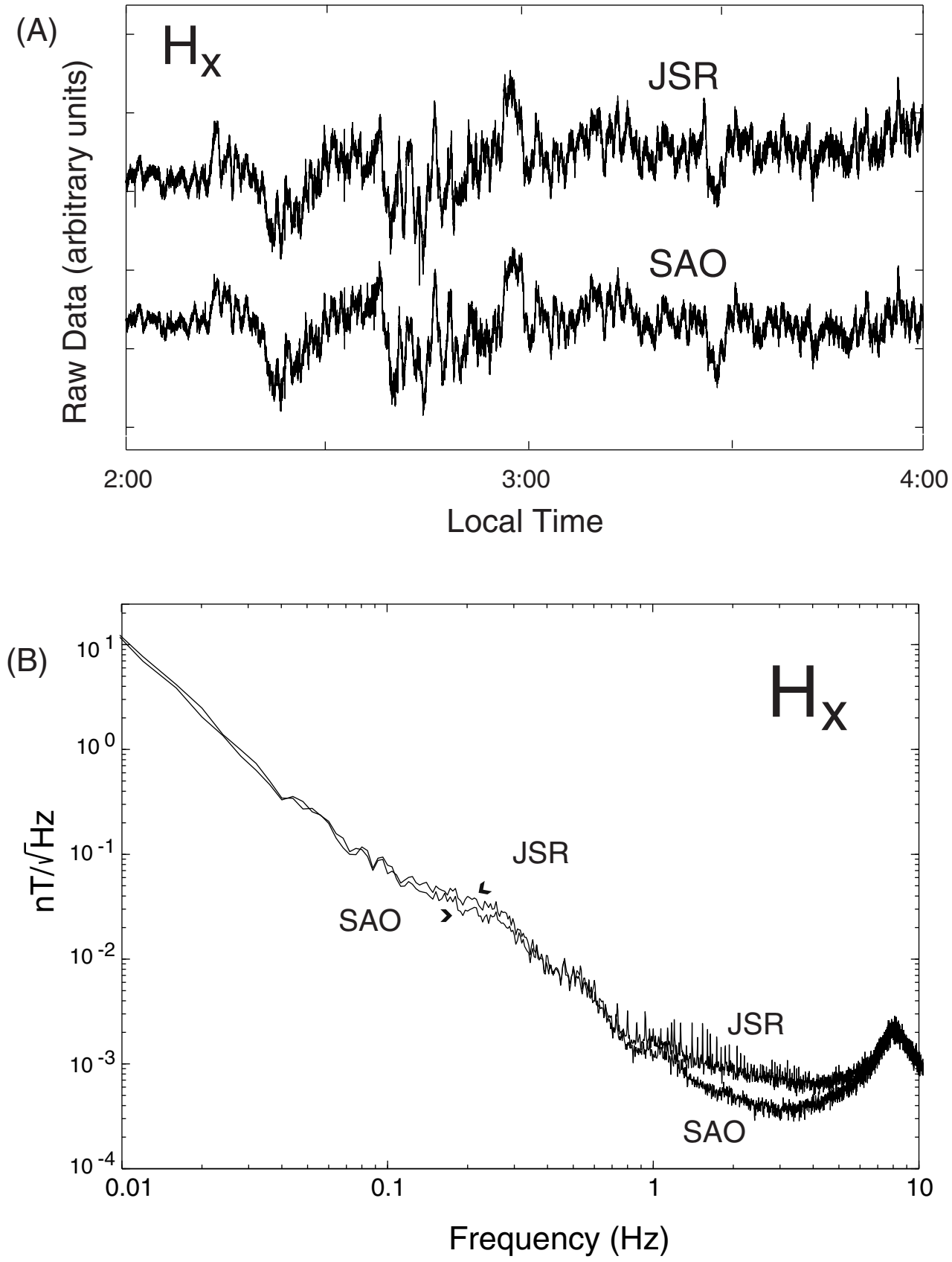

Figure 8. A. Raw data recorded at 40 sps on Hx at both JSR and SAO at 2:00 am local time. The traces are offset for presentation purposes and plotted in arbitrary units. B. Representative power spectra from JSR and SAO from 2:00-4:00 am local time.

most likely reflects JSR's close proximity to the Bay Area, a sprawling urban center, in contrast to SAO, a more isolated station where we see little, if any, BART signals.

CONCLUSION

Modern equipment makes the establishment of permanent EM observatories a straightforward prospect, and has allowed us to develop a prototype transportable system of sufficient quality to search for earthquake related EM field changes, particularly those preceding earthquakes. We will continue to monitor the performance of the ULF system and to build a library of continuous records in a variety of conditions in an attempt to understand potential sources of the variations in magnetic, electric, and seismic signals. Such familiarity with the system response to identifiable noise sources will provide a well-defined context in which potential future anomalies may be distinguished. A second, remote system is being prepared so that we are able deploy our equipment following a future large earthquake. In the future, more robust methods will be developed for handling large amounts of data and discriminating local anomalous signals.

ACKNOWLEDGMENTS

This research was supported by grants from NEHRP-U.S. Geological Survey (1434-HQ-97-GR-03105), Stanford Office of Technology and Licensing, and Stanford School of Earth Sciences McGee awards. We thank the Northern California Earthquake Data Center and the Seismological Laboratory at UC Berkeley for use of data from the reference station SAO. We thank Malcolm Johnston for his helpful review of the manuscript, and we greatly appreciate the technical support provided by Tom Liu, Russell

Sell and Bill Trabucco, and the generous field assistance of Danielle Boyd, Seth Haines, Joern Hoffmann, Sigurjon Jonsson, Sharon Kedar, Erminia Mallia-Zarb, and John Townend.

REFERENCES

Bernardi, A., A.C. Fraser-Smith, P.R. McGill, and O. G. Villard, Jr. (1991). Magnetic field measurements near the epicenter of the Ms 7.1 Loma Prieta earthquake, *Phys. Earth Planet. Int.* **68**, 45-63.

Campbell, W.H. (1969). Concurrent equatorial and high-latitude geomagnetic pulsations, *Radio Science* **4,** 859.

Dibblee, Jr., T.W. (1966). Geologic map of the Palo Alto 15-minute quadrangle, California, *U.S. Geological Survey*, scale 1:62500.

Draganov, A.B., U.S. Inan, and Y.N. Taranenko (1991). ULF magnetic signatures at the earth due to groundwater flow: A possible precursor to earthquakes*, Geophys. Res. Lett*. **18**, 1127-1130.

Fenoglio, M.A., M. J. S. Johnston, and J. D. Byerlee (1995). Magnetic and electric fields associated with changes in high pore pressure in fault zones: Application to the Loma Prieta ULF emissions, *J. Geophys. Res.* **100**, 12,951-12,958.

Fraser-Smith, A. C. (1993). Analysis of low-frequency electromagnetic field measurements near the epicenter, Loma Prieta, California, Earthquake of October 17, 1989; Preseismic observations*, U.S. Geol. Survey Prof. Paper 1550-C*, C17-C251.

Fraser-Smith, A.C., A. Bernardi, P.R. McGill, M.E. Ladd, R.A. Helliwell, and O.G. Villard, Jr. (1990). Low-frequency magnetic measurements near the epicenter of the M_s 7.1 Loma Prieta earthquake, *Geophys. Res. Lett.* **17**, 1465-1468.

Fraser-Smith, A.C. and J.L. Buxton (1975). Superconducting magnetometer measurements of geomagnetic activity in the 0.1- to 14-Hz frequency range, *J. Geophys. Res*. **80**, 3141-3147.

Fraser-Smith, A.C and D.B. Coates (1978). Large amplitude ULF electromagnetic fields from BART, *Radio Science* **13**, 661-668.

Gokhberg, M.B., V.A. Morgounov, T. Yoshino, and I. Tomizawa (1982). Experimental measurement of electromagnetic emissions possibly related to earthquakes in Japan, *J. Geophys. Res*. **87**, 7824-7828.

Hayakawa, M., R. Kawate, O. A. Molchanov, and K. Yumoto (1996). Results of ultra-low-frequency magnetic field measurements during the Guam earthquake of 8 August 1993, *Geophys. Res. Lett.* **23**, 241-244.

Jacobs, J.A. (1970). *Geomagnetic micropulsations*, New York, Springer, 179 pp.

Johnston, M.J.S. (1989). Review of magnetic and electric field effects near active faults and volcanoes in the U.S.A., *Phys. Earth Planet. Int.* **57**, 47-63.

Johnston, M.J.S. (1997). Review of electric and magnetic fields accompanying seismic and volcanic activity, *Surveys in Geophysics* **18**, 441-475.

Johnston, M.J.S. and R.J. Mueller (1987). Seismomagnetic observation with the July 8, 1986, ML 5.9 North Palm Springs earthquake, *Science* **237**, 1201-1203.

Johnston, M.J.S., R.J. Mueller, and Y. Sasai (1994). Magnetic field observations in the near-field of the 28 June 1992 M7.3 Landers California, earthquake, *Bull. Seism. Soc. Am*. **84**, 792-798.

Kopytenko, Yu.A., T.G. Matiashvili, P.M. Voronov, E.A. Kopytenko, and O.A. Molchanov (1993). Detection of ultra-low frequency emissions connected with the Spitak earthquake and its aftershock activity, based on geomagnetic pulsations data at Dusheti and Vardzia observatories, *Phys. Earth Planet. Int.* **77**, 85-95.

Lighthill, J., ed. (1996). *A critical review of VAN, earthquake prediction from seismic electrical signals*, River Edge, New Jersey, World Scientific Publishing Company, 376 pp.

Liu, T.T. and A.C. Fraser-Smith (1997). Hayward fault earthquake prediction project: ULF magnetic field measurements, *Technical Report WO8035-02, Electric Power Research Institute*, 57 pp.

Liu, T.T. and A.C. Fraser-Smith (1998). Identification and Removal of Man-Made Transients from Geomagnetic Array Time Series: A Wavelet Transform Based Approach, To appear in the Proceedings of the 32nd Asilomar Conference on Signals, Systems, and computers.

Longuet-Higgins, M.S. (1950). A theory of the origin of microseisms, *Phil. Trans. A.* **243**, 1-35.

Molchanov, O.A., Yu. A. Kopytenko, P.M. Voronov, E.A. Kopytenko, T.G. Matiashvili, A.C. Fraser-Smith, and A. Bernardi (1992). Results of ULF Magnetic field measurements near the epicenters of the Spitak (Ms=6.9) and Loma Prieta (Ms=7.1) earthquakes: comparative anaysis, *Geophys. Res. Lett.* **19**, 1495-1498.

Merzer, M. and S.L. Klemperer (1997). Modeling low-frequency magnetic-field precursors to the Loma Prieta earthquake with a precursory increase in fault-zone conductivity, *PAGEOPH* **150**, 217-248.

Park, S.K. (1991). Monitoring resistivity changes prior to earthquakes in Parkfield, California, with telluric arrays, *J. Geophys. Res*. **96**, 14211-14237.

Park, S.K. (1996). Precursors to earthquakes: Seismoelectromagnetic signals, *Surveys in Geophysics* **17**, 493-516.

Park, S.K., M. J.S. Johnston, T. R. Madden, F. D. Morgan, H. F. Morrison (1993). Electromagnetic precursors to earthquakes in the ULF band: A review of observations and mechanisms, *Reviews of Geophysics* **31**, 117-132.

Parrot, M. and M.J.S. Johnston, eds. (1989). Seismoelectromagnetic effects, *Phys. Earth Planet. Int.* **57**, 177 pp.

Pham, V.-N., D. Boyer, J. -L. Mouel, G. Chouliaras, and G.N. Stavrakakis (1999). Electromagnetic signals generated in the solid Earth by digital transmission of radio-waves as a plausible source for some so-called 'seismic electric signals', *Phys. Earth Planet. Int.* **114**, 141-163.

Roeloffs, E.A., D.C. Agnew, and D.V. Fitterman (1996). U.S. Geological Survey plan and guidelines for monitoring of electromagnetic signals related to earthquakes, FY1996-FY2000, *USGS-OFR*.

Tascione, T.F. (1994). *Introduction to the space environment*, Malabar, Florida, Kreiger Publishing Company, 151 pp.

Telford, W.M., L.P. Geldart, and R.E. Sheriff (1990). *Applied Geophysics (Second Edition)*, New York, Cambridge University Press, 770 pp.

Uhrhammer, R. A., W. Karavas, and B. Romanowicz (1998). Broadband seismic station installation guidelines, *Seism. Res. Lett.* **69**, 15-26.

Uyeda, S., T. Kudo, K. Hattori, T. Yamaguchi, Y. Orihara, K. Sayanagi, I. Takahashi, Y. Noda, T. Tanbo, T. Nagao, and K. Kawabata (1998). Geoelectric potential measurement study in Japan: General and the latest results, *RIKEN/NASDA Workshop on Seismo-ULF Emissions, December 14-16, 1998*, NASA, EORC, Roppongi, Tokyo.

Varotsos P., K. Alexopoulos, and M. Lazaridou (1993a). Latest aspects of earthquake prediction in Greece based on seismic electric signals, II, *Tectonophysics* **224**, 1-37.

Varotsos, P.K., K. Alexopoulos, M. Lazaridou-Varosou, and T. Nagao (1993b). Earthquake predictions issued in Greece by seismic electric signals since February 6, 1990, *Tectonophysics* **224**, 269-288.

Warwick, J.W., C. Stoker, and T.R. Meyer (1982). Radio emission associated with rock fracture: Possible application to the great Chilean earthquake of May 22, 1960, *J. Geophys. Res.* **87**, 2851-2859.

Yoshino, T (1991). Low-frequency seismogenic electromagnetic emissions as precursors to earthquakes and volcanic eruptions in Japan, *J. Sci. Explor*. **5**, 121-144.